Structural Engineering and Mechanics, *Vol. 75, No. 4 (2020) 465-475*
DOI: https://doi.org/10.12989/sem.2020.75.4.465

The nonlinear galloping of iced transmission conductor under uniform and turbulence wind

Zhonghua Liu*, Chenhui Ding[a], Jian Qin[b] and Ying Lei[c]

School of Architecture and Civil Engineering, Xiamen University, 422 Siming South Road, Xiamen, China

(Received December 12, 2019, Revised February 19, 2020, Accepted February 20, 2020)

Abstract. The analytical approach for stability and response of iced conductor under uniform wind or turbulent wind is presented in this study. A nonlinear dynamic model is established to describe the motion of iced conductor galloping. In the case of uniform wind, the stability condition is derived by analyzing the eigenvalue associated with linearized matrix; The first order and second order approximation of galloping amplitude are obtained using multi-scale method. However, real wind has random characteristics essentially. To accurately evaluate the performance of the galloping iced conductor, turbulence wind should be described by random processes. In the case of turbulence wind, the Lyapunov exponent is conducted to judge the stability condition; The probability density of displacement is obtained by using the path integral method to predict galloping amplitude. An example is proposed to verify the effectiveness of the previous methods. It is shown that the fluctuating component of wind has little influence on the stability of iced conductor, but it can increase galloping amplitude. The analytical results on stability and response are also verified by numerical time stepping method.

Keywords: iced conductor; turbulence wind; galloping; multi-scale method; path integral method

1. Introduction

Galloping is a phenomenon caused by aerodynamic instability. As ice or wet snow accreting on transmission conductor in winter, it is expected that the conductor galloping may occur under strong wind. This phenomenon may lead to short circuit or ground fault of the transmission conductor, and resulting in instantaneous voltage drop. If galloping lasts for a long time, the supporting parts may be fatigued and broken, leading serious accident that the transmission conductor may fall down(Desai et al. 1995; Van Dyke and Laneville 2008). Due to the damage effect caused by the transmission conductor failure, it has a great impact on the power supply, which will cause serious damage. When iced conductors is under strong wind excitation, excessive vibration will occur due to self-weight and the tension of the conductor. The frequency of galloping phenomenon is relatively low, which is about 0.1 Hz ~3 Hz. The amplitude of galloping phenomenon is larger, which can be more than 1 times of its sag. The amplitude of galloping isdetermined by span, stiffness, tension of transmission conductor, icing shape and weight.

The galloping of iced transmission conductor was first described as one-degree-of-freedom model by Den Hartog(1932) in which the important conclusion was given that instability of the transmission conductor will occur if the slope of the lift is greater than the drag. Irvine and Caughey (1974) assumed that the horizontal cable has a parabolic shape in the equilibrium and studied the free vibration characteristics of the cable by using the linear theory. The twist freedom has been considered and it play a significant role as vertical freedom do for the initiation of galloping both in the work of Nigol’s two-degree-of-freedom vertical and torsional galloping mechanism(Nigol and Buchan 1981) and Yu’s three-degree-of-freedom model with eccentrically inertial coupling (Yu, Shah and Popplewell 1992). Based on those proposed mechanisms, some 3DOF analytical galloping models (Wang *et al* 1998; Yu *et al* 1993, Lou *et al* 2014) have been further developed to assess the stability of conductors and to obtain explicit expressions for the periodic and quasi-periodic solutions of galloping. In practice, the galloping problem always become more complicated such as involving geometric nonlinearities and nonlinear aeroelastic forces.

The effects of wind on cooling tower (Zhang *et al* 2019), suspension bridges (Petrini *et al* 2019) and super-tall buildings (Zhi *et al* 2015) have been studied widely in recent years. In order to simplify the study, the wind model is usually taken as uniform wind. In fact, the real wind should be regarded as turbulence wind and be treated as random process. Due to the complexity of the turbulence wind, numerical calculation and experimental methods are usually used in those studies (Choi *et al* 2015, Lin *et al* 2017). Usually only the uniform wind is concerned when it comes to galloping. But it is shown that turbulence in the wind affects galloping behavior significantly (Chadha and Jaster 1975). In order to study the influence of wind randomness on conductor’s galloping, the stability and

*Corresponding author, Professor
E-mail: liuzh@xmu.edu.cn
[a] M.Sc,
E-mail: d2012621@163.com
[b] M.Sc
E-mail: 1026467032@qq.com
[c] Professor
E-mail: ylei@xmu.edu.cn

http://www.techno-press.com/journals/sem&subpage=7
ISSN: 1225-4568 (Print), 1598-6217 (Online)

response of the iced transmission conductor under both uniform and turbulence wind are studied in this paper. Analytical results are obtained under turbulence wind are compared with those results under uniform wind. The galloping stability and amplitude are also verified through the galloping simulation under both uniform wind and the turbulence wind.

2. The motion equation of galloping iced conductor

The schematic configuration of a galloping iced transmission conductor under transverse horizontal (unidirectional) wind is shown in Fig. 1, where X and Y are span-wise coordinate and vertical coordinate of the iced conductor, respectively. Generally, galloping of iced conductor can be decomposed into three translational components in longitudinal, vertical and transverse horizontal motions and one torsional motion about the axis of the conductor. The motion in vertical direction is usually the most important according the observations and previous studies on galloping iced conductor. For simplicity, only the vertical displacement $v(x,t)$ was considered in the following.

Supposing that the static equilibrium configuration is represented through the parabolic profile:

$$y(x) = \frac{MgL^2}{2T}\left(\frac{x}{L} - \frac{x^2}{L^2}\right) \tag{1}$$

where T = the tension of the conductor in the static state along the axial direction; L= the span of the conductor and M = the mass per unit length of the iced conductor. Function $y(x)$ is a catenary function representing the initial cable configuration in its static equilibrium state (Nayfeh et at. 2002).

Lagrange's equation of motion under generalized coordinate system is given by

$$\frac{d}{dt}\left(\frac{\partial T}{\partial \dot{q}_y}\right) - \frac{\partial T}{\partial q_y} + \frac{\partial V}{\partial q_y} + \frac{\partial D}{\partial \dot{q}_y} = F_y \tag{2}$$

where T, V and D = kinetic energy, potential energy and dissipative energy of the system, respectively; and F_y = generalized aerodynamic force; q_y =generalized displacement. The total kinetic energy is calculated by integration along the line span as

$$T = \int_0^L \frac{1}{2} M\dot{v}^2\, dx \tag{3}$$

The total potential energy of the iced conductors can be expressed in terms of elastic strains

$$V = \int_0^L \frac{1}{2} EA\varepsilon_s^2\, dx + \int_0^L T\varepsilon_s\, dx + V_g \tag{4}$$

where EA=axial stiffness of the conductor; ε_s = nonlinear axial strain. The transmission conductor is a typical flexible structure such that Lagrange's strain without considering bending stiffness is usually used to describe the nonlinear axial deformation when galloping occurs(Yu *et al*. 1993). Because only the vertical motion is considered, the axial nonlinear strain of the line can be approximated written in terms of vertical components as

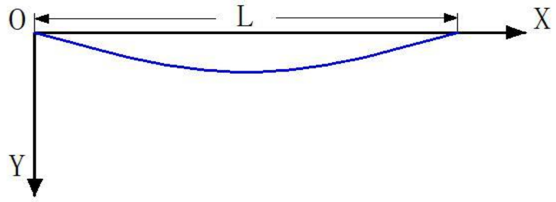

Fig. 1 Configuration of iced conductor

$$\varepsilon_s \approx \frac{dy}{dx}\frac{\partial v}{\partial x} + \frac{1}{2}\left(\frac{\partial v}{\partial x}\right)^2 \tag{5}$$

The gravitational potential energy V_g can be expressed as

$$V_g = \int_0^L -Mgv\, dx \tag{6}$$

The dissipative function D represents the actions of dissipative forces on the system. Assuming a linear damping mechanism for the iced conductors leads to the following expression

$$D = \frac{1}{2}\int_0^L 2M\omega_y\xi_y\dot{v}^2\, dx \tag{7}$$

where ξ_y= the viscous damping ratio of the conductor and ω_y= the associated free vibration frequencies.

The displacement $v(x,t)$ in the vertical direction can be expressed as the product of the generalized displacement $q_y(t)$ and associated mode shapes $\phi(x)$. For simplicity, we assume that the iced conductor is dominated only by one vertical mode. According to the Galerkin method, the vertical displacement $v(x,t)$ can be written in the form

$$v(x,t) = \phi(x)q_y(t). \tag{8}$$

Substituting Eqs.(3-8) into Eq. (2), the equation of motion for the iced conductor are obtained as:

$$a_1\ddot{q}_y(t) + a_2\dot{q}_y(t) + a_3q_y(t) + a_4q_y(t)^2 + a_5q_y(t)^3 = F_y(t) \tag{9}$$

where $a_1, \dots, a_5$ = coefficients given in the appendix; $F_y(t)$ = the generalized aerodynamics forces, which can be conducted by the following processes.

Suppose that the wind is in the transverse horizontal direction. According to the quasi-steady assumption, the aerodynamic force $f_y(x,t)$ per unit length of the iced conductor are described by

$$f_y(x,t) = \frac{1}{2}\rho U^2 DC_y(\alpha) \tag{10}$$

where ρ = air density, D and $C_y(\alpha)$ = the diameter and vertical aerodynamics coefficient of the iced conductor, respectively. U = the uniform wind velocity.

The aerodynamic force of the iced conductor depends on the instantaneous wind attack angle, which can be written as

$$\alpha = \theta_0 - \alpha_0 = \theta_0 - \frac{\dot{v}}{U} \tag{11}$$

with

$$\alpha_0 = \frac{\dot{v}}{U} \tag{12}$$

where θ_0 is the initial wind attack angle and $\dot{v}$ means the vibration velocity in the vertical direction. The vertical aerodynamics coefficient of the iced conductor $C_y(\alpha)$ can be obtained as

$$C_y(\alpha) = C_L(\alpha)\cos(\alpha_0) - C_D(\alpha)\sin(\alpha_0) \tag{13}$$

with $C_L(\alpha)$ and $C_D(\alpha)$ =lift and drag coefficients, respectively, which are available by the wind tunnel experiments at each wind angle α_0.

It is convenient to rewrite the aerodynamics coefficient $C_y(\alpha_0)$ in the following form:

$$C_y(\alpha_0) = h_0 + h_1\alpha_0 + h_2\alpha_0^2 + h_3\alpha_0^3 \tag{14}$$

The coefficients h_{0-3} can be obtained by wind tunnel experiments or computer simulations. The aerodynamics coefficient $C_y(\alpha_0)$ is affected by initial wind attack angle and configures of ice on the conductor.

The generalized aerodynamics forces $F_y(t)$ in Eq. (9) can be given as the form

$$F_y(t) = \int_0^L f_y(x,t)\,\phi(x)\,dx \tag{15}$$

The term associated with h_0 can only cause static figuration, so we omitted its effects. Let $y(t)= q_y(t)$, Eq. (9) is rewritten as

$$\ddot{y} + c\dot{y} + k_1 y + k_2 y^2 + k_3 y^3 = b_1\dot{y} + b_2\dot{y}^2 + b_3\dot{y}^3 \tag{16}$$

All coefficients in Eq. (16) are given in the appendix.

By introducing the state space variable vector $\boldsymbol{y} = [y_1, y_2]^T = [y, \dot{y}]^T$, Eq. (16) can be rewritten in the form of first-order differential equations as

$$\dot{y}_1 = y_2 \tag{17}$$

$$\dot{y}_2 = -cy_2 - k_1y_1 - k_2{y_1}^2 - k_3{y_1}^3 + b_1y_2 + b_2{y_2}^2 + b_3{y_2}^3 \tag{18}$$

These dynamic equations are obtained in the case that the wind is regard as uniform wind, that is, only the mean wind velocity is considered. In fact, the turbulent wind model is more realistic and it can account for the fluctuating effects of wind. The turbulent wind velocity can usually be decomposed into its mean wind velocity and fluctuating apart. The turbulent wind velocity $\widetilde{U}(t)$ is a time-variable random process (Lin and Cai 1995) and modelled as

$$\widetilde{U}(t) = U(t) + u(t) = U(t)(1 + W(t)) \tag{19}$$

In which, $U(t)$ denotes the mean wind velocity, and $u(t)$ is the random fluctuation wind velocity. The fluctuation wind velocity is simplified as Gaussian white noise $W(t)$ with intensity γ^2. Parameter γ^2 should be small enough to ensure the turbulent wind velocity $\widetilde{U}(t)$ remains positive, which means the wind has an invariable direction.

Since the root-mean square value of the turbulence rarely exceeds 30 percent of the mean velocity, it is reasonable to have the following approximation:

$$1/\widetilde{U}(t) = (1 - W(t))/U(t) \tag{20}$$

Substituting the uniform wind velocity U in Eq. (10) by random turbulent wind velocity $\widetilde{U}(t)$ in Eq. (19), the dynamic equation (16) can be written as the following dynamic equation:

$$\ddot{Y} + c\dot{Y} + k_1Y + k_2Y^2 + k_3Y^3 = b_1\dot{Y} + b_2\dot{Y}^2 + b_3\dot{Y}^3 + b_1\dot{Y}W(t) - b_3\dot{Y}^3W(t) \tag{21}$$

where $Y(t)$ is a random process representing the vertical displacement. Considering new state space variable $\boldsymbol{Y} = [Y_1, Y_2]^T = [Y, \dot{Y}]^T$, the dynamic equation for $\boldsymbol{Y}$ can be written as

$$\dot{Y}_1 = Y_2 \tag{22}$$

$$\dot{Y}_2 = -cY_2 - k_1Y_1 - k_2{Y_1}^2 - k_3{Y_1}^3 + b_1Y_2 + b_2Y_2^2 + b_3Y_2^3 + b_1Y_2W(t) - b_3Y_2^3W(t) \tag{23}$$

Eqs. (22) and (23) can be regard as Stratonovich differential equations of the system. Introducing the Wong-Zakai correction terms, the Itô differential equations can be derived as:

$$dY_1 = Y_2dt, \tag{24}$$

$$dY_2 = \left(-(c - b_1)Y_2 - k_1Y_1 - k_2{Y_1}^2 - k_3{Y_1}^3 + b_2Y_2^2 + b_3Y_2^3 + \frac{1}{2}\gamma^2(b_1Y_2 + b_3Y_2^3)(b_1 + 3b_3Y_2^2)\right)dt + \sqrt{b_1^2\gamma^2Y_2^2 + b_3^2\gamma^2Y_2^6}\,dB(t), \tag{25}$$

where $B(t)$ is a standard unit Wiener process. It is convenient to analyze the stability and responses of the iced conductor using Itô differential equations (24) and (25).

3. Stability and response of iced conductor under uniform wind

The stability and response of iced conductor under uniform wind are studied in this section.

3.1 Stability analysis

For system as described in Eqs.(17) and (18), the stability depends on it's linear system(Macdonald and Larose 2006). Obviously, the state space variable $\boldsymbol{Y} = 0$ is an equilibrium point of the dynamical system. The linearized system on the equilibrium point can be written as

$$\dot{\mathbf{y}} = \boldsymbol{A}\mathbf{y}, \boldsymbol{A} = \begin{bmatrix} 0 & 1 \\ -k_1 & -c + b_1 \end{bmatrix} \tag{26}$$

Based on the Lyapuov first-order approximation theory, the initial stability of a nonlinear system is governed by the eigenvalues of linearized matrix $\boldsymbol{A}$. If the real part of all eigenvalue of $\boldsymbol{A}$ is negative, the system remains stable; otherwise, the system becomes unstable. Generally speaking, it is difficult to obtain analytical solution of eigenvalues associated with a multi-dimensional matrix $\boldsymbol{A}$. The Routh-Hurwitz stability criterion can be used to derive stability criterion, which is stated in terms of the coefficients of the characteristic equation instead of the eigenvalues associated with the linearized matrix. The characteristic equation of the linearized matrix $\boldsymbol{A}$ is

$$\lambda^2 + (c - b_1)\lambda + k_1 = 0 \tag{27}$$

where λ is the eigenvalue of matrix $\boldsymbol{A}$. The eigenvalues is easily obtained as

$$\lambda = \left(-\frac{c - b_1}{2}\right) \pm \frac{\sqrt{(c - b_1)^2 - 4k_1}}{2} \tag{28}$$

The sufficient and necessary condition for stability of the dynamical system in Eqs. (17) and(18) is given by

$$c - b_1 > 0 \tag{29}$$

Considering coefficients c and b_1, the criterion mean wind velocity U_r can be conducted as

$$U_r = \frac{c}{\frac{1}{2}\rho D \hbar_1 \int_0^L sin^2(\frac{\pi x}{L})dx} = \frac{4M\omega_y\xi_y}{\rho D \hbar_1} \tag{30}$$

If the uniform wind velocity $U < U_r$, the iced conductor is stable; otherwise, if the wind velocity $U > U_r$, the galloping occurs. The result coincides with that of the Den Hartog theory.

3.2 Response of the iced conductor galloping

When wend velocity exceeds the criterion wend velocity, the iced conductor will oscillate seriously with large amplitude. The occurrence of galloping could cause large dynamics tension acting on transmission conductors and towers and may bring damage of fittings, illustrator strings, tower components, and even the collapse of whole tower. For nonlinear system the multi-scale method(Nayfeh and Mook 1995) is a powerful analytical method to obtained response amplitude.

Based on the observation of Galloping, the oscillation the iced conductors usually form a limited circle. For one-degree-of-freedom system described in Eq. (16), it can be written as the following weak nonlinear form:

$$\begin{aligned}\ddot{y} + \omega_y^2 y = -k_2 y^2 - k_3 y^3 + (b_1 - c)\dot{y} + b_2\dot{y}^2 \\ + b_3\dot{y}^3 = \varepsilon f(y, \dot{y})\end{aligned} \tag{31}$$

where a dimensionless perturbation parameter $\varepsilon \ll 1$ is introduced. New independent variables t,εt,$\varepsilon^2 t$, are the different time scales, and introduce the following new variables:

$$T_n = \varepsilon^n t \tag{32}$$

The derivatives with respect to *t* become expansions in terms of the partial derivatives with respect to the T_n according to

$$\frac{d}{dt} = \frac{dT_0}{dt}\frac{\partial}{\partial T_0} + \frac{dT_1}{dt}\frac{\partial}{\partial T_1} + \cdots = D_0 + \varepsilon D_1 + \cdots \tag{33}$$

$$\frac{d^2}{dt^2} = D_0^2 + 2\varepsilon D_0 D_1 + \cdots \tag{34}$$

The solution *y* can be represented by an expansion as

$$y(t) = y_0(T_0, T_1,\cdots) + \varepsilon y_1(T_0, T_1,\cdots) + \cdots \tag{35}$$

Substituting those equations into Eq. (16) and equating the coefficient of ε^0 and ε^1 to zero, we have

$$D_0^2 y_0 + \omega_y^2 y_0 = 0 \tag{36}$$

$$D_0^2 y_1 + \omega_y^2 y_1 = -2D_0 D_1 y_0 + f(y_0, D_0 y_0) \tag{37}$$

It is convenient to write the general solution of Eq. (36) in the complex form

$$y_0 = A(T_1)\exp(i\omega_y T_0) + \bar{A}(T_1)\exp(-i\omega_y T_0) \tag{38}$$

The function A is still arbitrary at this level of approximation, and it can be determined by eliminating the secular terms at the higher levels of approximation.

Substituting y_0 into Eq. (37) leads to

$$\begin{aligned}D_0^2 y_1 + \omega_y^2 y_1 = -2i\omega_y D_1 A \exp(i\omega_y T_0) \\ - k_2[A^2\exp(2i\omega_y T_0) + A\bar{A}] \\ -k_3[A^3\exp(3i\omega_y T_0) + 3A^2\bar{A}\exp(i\omega_y T_0)] \\ + (b_1 - c)i\omega_y A\exp(i\omega_y T_0) \\ +b_2[-\omega_y^2 A^2\exp(2i\omega_y T_0) + \omega_y^2 A\bar{A}] \\ +b_3[-i\omega_y^3 A^3\exp(3i\omega_y T_0) + 3i\omega_y^3 A^2\bar{A}\exp(i\omega_y T_0)] \\ + cc.\end{aligned} \tag{39}$$

where *cc* denotes the complex conjugate of the preceding terms. Any particular solution of (39) has a secular term containing the factor $T_0\exp(i\omega_y T_0)$ unless

$$\begin{aligned}2i\omega_y D_1 A = -k_3(3A^2\bar{A}) + (b_1 - c)\, i\omega_y A \\ + b_3(3i\omega_y^3 A^2\bar{A})\end{aligned} \tag{40}$$

In solving equations having the form of (40), we find it convenient to write A in the polar form

$$A = \frac{1}{2}a(T_1)\exp(i\beta(T_1)) \tag{41}$$

where a and β are real functions of T_1. Substituting Eq. (41) into Eq. (40) and separating the result into real and imaginary parts, we obtain

$$a' = \frac{1}{2}(b_1 - c)a + \frac{3}{8}b_3\omega_y^2 a^3 \tag{42}$$

$$\beta' = \frac{3}{8}\frac{k_3}{\omega_y}a^2 \tag{43}$$

where the prime denotes the derivative with respect to T_1. It follows that

$$\beta = \frac{3}{8}\frac{k_3}{\omega_y}a^2 T_1 + \beta_0 \tag{44}$$

where β_0 is a constant. If the iced conductor can vibrate with a limited stationary amplitude, the amplitude can be obtained by setting $a' = 0$. The amplitudes are

$$a = 0; \pm\sqrt{r}\,, r = 4(c - b_1)/3b_3\omega_y^2 \tag{45}$$

It is seen that the amplitude a depends on the value of r. when $r < 0$, the amplitude a is 0. It means the system is stable if $r < 0$. Meanwhile the nonzero amplitude $\sqrt{r}$ exists only if $r > 0$. Considering the stability condition in Eq. (29), the galloping occurs with limited amplitude only under the condition $b_3 < 0$. That is, the galloping with limited amplitude occurs only if the coefficient $h_3 < 0$ in Eq. (14).

Returning to Eq. (41), we find that

$$A = \frac{1}{2} a \exp\left(i \frac{3}{8} \frac{k_3}{\omega_y} a^2 T_1 + i\beta_0\right) \tag{46}$$

The first approximation of y is

$$y_0 = a\cos(\phi)\,, \phi = \omega_y t + \frac{3}{8}\frac{k_3}{\omega_y} a^2 t + \beta_0 \tag{47}$$

With secular term is zero, y_1 can also be solved from Eq. (39) as

$$\begin{aligned} y_1 = &-\frac{k_2\left[3A\bar{A} - A^2\exp(2i\omega_y T_0)\right]}{3\omega_y^2} \\ &- \frac{k_3\left[-A^3\exp(3i\omega_y T_0)\right]}{8\omega_y^2} \\ &+b_2\omega_y^2 \frac{\left[3A\bar{A} + A^2\exp(2i\omega_y T_0)\right]}{3\omega_y^2} \\ &+ b_3\omega_y^3 \frac{\left[iA^3\exp(3i\omega_y T_0)\right]}{8\omega_y^2} + cc \end{aligned} \tag{48}$$

Considering Eq. (35), the second order approximation of y is

$$\begin{aligned} y = a\cos(\phi) &- \frac{k_2}{k_1}\left[\frac{1}{2}a^2 - \frac{1}{6}a^2\cos(2\phi)\right] \\ &- \frac{k_3}{k_1}\left[-\frac{1}{32}a^3\cos(3\phi)\right] \\ &+b_2\left[\frac{1}{2}a^2 + \frac{1}{6}a^2\cos(2\phi)\right] + b_3\left[-\frac{1}{32}\omega_y a^3\sin(3\phi)\right] \end{aligned} \tag{49}$$

It is seen that the solution contains harmonic vibrations and two constant terms. Those terms about y^2 and $\dot{y}^2$ can make the midpoint of the motion drifted with respect to the initial configuration.

4. Stability and response of iced conductor under turbulent wind

The turbulent wind velocity can be decomposed as mean wind velocity and fluctuant wind velocity as shown in Eq. (19). In this Section, the effects of fluctuating wind on stability and response of iced conductor galloping are discussed.

4.1 Stability analysis

The equilibrium point of the random dynamical system (21) is $\boldsymbol{Y} = 0$. The linearized system on this equilibrium point can be written as

$$\ddot{y} + (c - b_1)\dot{y} + k_1 y - b_1\dot{y}\mathrm{W}(t) = 0 \tag{50}$$

Considering the Wong-Zakai correction terms, The Itô differential equations associated with Eq. (50) are

$$\begin{cases} y_1' = y_2 \\ dy_2' = (-\omega_y^2 y_1 - (c - b_1 - \frac{1}{2}b_1^2\gamma^2)y_2)dt + \sqrt{b_1^2\gamma^2 y_2^2}\,dB(t) \end{cases} \tag{51}$$

Let

$$y_1 = A(t)\cos\theta, y_2 = -A(t)\omega_y\sin\theta\,, \theta = \omega_y t + \varphi(t) \tag{52}$$

The amplitude $A(t)$ can then be expressed as

$$A(t) = \sqrt{y_1^2 + y_2^2/\omega_y^2} \tag{53}$$

and the following partial derivatives are obtained

$$\frac{\partial A}{\partial y_1} = \cos\theta, \frac{\partial A}{\partial y_2} = \frac{\cos\theta}{\omega_y}, \frac{\partial^2 A}{\partial y_2^2} = \frac{\cos^2\theta}{A\omega_y^2} \tag{54}$$

Using Itô differential rule to obtain an Itô equation for amplitude $A(t)$, and applying the time averaging for the drift and diffusion coefficients, we obtain the averaged Itô equation (Cai and Zhu 2017)

$$dA = m(A)dt + \sigma(A)dB(t) \tag{55}$$

with

$$\begin{aligned} m(A) = \frac{1}{2\pi}\int_0^{2\pi} &\left[-\left(c - b_1 - \frac{1}{2}b_1^2\gamma^2\right)A\cos^2\theta \right. \\ &\left. + \frac{1}{2}b_1^2\gamma^2 A\sin^2\theta\cos^2\theta\right] d\theta \end{aligned} \tag{56}$$

$$= -\tfrac{1}{2}(c - b_1)A + \tfrac{5}{16}b_1^2\gamma^2 A$$

$$\sigma^2(A) = \frac{1}{2\pi}\int_0^{2\pi}[b_1^2\gamma^2 A^2\sin^4\theta]d\theta = \frac{3}{8}b_1^2\gamma^2 A^2 \tag{57}$$

Based on the Oseledect multiplicative ergodic theorem, the necessary and sufficient condition for the asymptotic stability with probability one of the trivial solution of the system is that the largest Lyapunov exponent of the linearized equation of the system is negative. The Lyapunov exponent of the linearized equation is derived as

$$\lambda = m'(0) + \frac{1}{2}[\sigma'(0)]^2 = -\frac{1}{2}(c - b_1) + \frac{1}{8}b_1^2\gamma^2 \tag{58}$$

Thus, the necessary and sufficient condition for the asymptotic stability with probability one of the trivial solution of system can be obtained approximately by letting the Lyapunov exponent in Eq. (58) to be negative, it is

$$\begin{aligned} \frac{2\left(-\sqrt{1+\gamma^2 c} - 1\right)}{\gamma^2} < b_1 < \frac{2\left(\sqrt{1+\gamma^2 c} - 1\right)}{\gamma^2} \\ \approx c - \frac{\gamma^2 c^2}{4} \end{aligned} \tag{59}$$

for small values of γ^2 and c. It is shown that the random fluctuation wind with weak intensity γ^2 has little effect on iced conductor galloping. The critical galloping velocity of mean wind is

$$U_r \approx \frac{c(1-\frac{\gamma^2 c}{4})}{\frac{1}{2}\rho D \hbar_1 \int_0^L sin^2(\frac{\pi x}{L})dx} \tag{60}$$

Because $\gamma^2 c \ll 1$ in Eq. (60), the effect of fluctuating wind on critical mean wind velocity is also small.

4.2 Response of the iced conductor Galloping

It is assumed that the equation of motion governed by Eqs.(24) and (25) are described in the form:

$$dY_i = a_i(Y_i)dt + b_i(Y_i)dB(t), i = 1,2 \tag{61}$$

with the following drift coefficient a_i and diffusion coefficient b_i:

$$a_1 = Y_2, b_1 = 0, b_2 = \sqrt{b_1^2\gamma^2 Y_2^2 + b_3^2\gamma^2 Y_2^6},$$

$$a_2 = -(c-b_1)Y_2 - k_1Y_1 - k_2{Y_1}^2 - k_3{Y_1}^3 + b_2Y_2^2 + b_3Y_2^3 + \frac{1}{2}\gamma^2(b_1Y_2 + b_3Y_2^3)(b_1 + 3b_3Y_2^2).$$

In which, Y_1 and Y_2 are the 2-dimensional state vector processes, and $B(t)$ is a standard unit Wiener process. For solving Eq. (61), the following high accuracy Runge- Kutta-Maruyama approximation is adopted:

$$Y_i = Y_{t'} + r(Y_{t'})\Delta t + b(Y_{t'})\Delta B_{t'} \tag{62}$$

where $t = t' + \Delta t$. Since the Winner process has independent increments, it follows from (62) that the sequence $Y_{n\Delta t}$ is a Markov chain. For sufficiently small Δt, this Markov chain will approximate the continuous time Markov process solution of the Itô differential Eq. (61).

The Path Integral (PI) method (Naess A. and Moe v. 2000) is based on the fact that the state vector Y_i obtained as a solution of Eq. (61) is a Markov vector process. This makes it possible to use a time stepping procedure to produce the joint probability density function $p(Y_1, Y_2, t)$ as a function of time *t* by exploiting the fundamental equation:

$$p(Y_1, Y_2, t) = \int_R p(Y_1, Y_2, t | Y'_1, Y'_2, t') p(Y'_1, Y'_2, t') dY'_1 dY'_2 \tag{63}$$

where $p(Y_1, Y_2, t | Y'_1, Y'_2, t')$ denotes the conditional probability density function of $\boldsymbol{Y}$ given that $Y_{t'} = Y'$. For small time increments $\Delta t = t - t'$, $p(Y, t | Y', t')$ will be referred to as the short time transition probability density. The short time transition probability density $p(Y_1, Y_2, t | Y'_1, Y'_2, t')$ can be always be given as an analytical and closed form expression. It is also observed from Eq. (61) that $p(Y_1, Y_2, t | Y'_1, Y'_2, t')$ is a Gaussian probability density function. Here the following forms are used:

$$p(Y_1, Y_2, t | Y'_1, Y'_2, t') = \delta(Y_1 - Y_1' - r_1(Y')\Delta t) \cdot \tilde{p}(Y_2, t | Y', t') \tag{64}$$

where $\delta(\cdot)$ denotes the Dirac delta function and

$$\tilde{p}(Y_2, t | Y', t') = \frac{1}{\sqrt{2\pi b_2(Y')^2 \Delta t}} exp\left\{-\frac{(Y_2 - Y_2' - r_2(Y')\Delta t)^2}{2b_2(Y')^2\Delta t}\right\} \tag{65}$$

Hence, $p(Y_1, Y_2, t | Y'_1, Y'_2, t')$ is a degenerate 2-dimensional Gaussian probability density function.

If the initial probability density function $p(Y, 0)$ is given, then, Eq. (61) can be invoked repeatedly to produce the time evolution of $p(Y_1, Y_2, t)$. If the response exists a stationary probability density function $p_s(Y_1, Y_2)$, $p(Y_1, Y_2, t)$ will approach this stationary probability density function with sufficient time. If the displacement Y_1 are concerned, the transient displacement probability density function and stationary displacement probability density function for Y_1 can also be obtained as

$$p(Y_1, t) = \int_{-\infty}^{\infty} p(Y_1, Y_2, t) dY_2 \tag{66}$$

$$p_s(Y_1) = \int_{-\infty}^{\infty} p_s(Y_1, Y_2) dY_2 \tag{67}$$

The response of the iced conductor can be predicted using its displacement probability density function.

5. Example

In this example, the structural parameters of the iced conductor were listed in table 1. For simplicity, the aerodynamics coefficients in Y direction was $C_y(\alpha_0) = -0.531 + 3.544\alpha_0 + 1.826\alpha_0^2 - 3.329\alpha_0^3$ with initial wind attack angle $\theta_0 = \pi/6$ and the air density $\rho = 1.293Kg/m^3$.

The critical wind velocity of the galloping iced conductor under uniform wind was conducted as U_r=1.76m/s. The result was confirmed with digital simulation where the fourth order Runge-Kutta method was used for computing Eq. (17)-(18). The vertical displacement with different wind velocities were shown in Fig. 1. Fig. 1(a) shows the vertical displacement with U=1.6m/s. It is shown that the amplitude of the conductor tends to zero in sufficient long time. The galloping do not occur when the wind velocity less than critical velocity. However, when the wind velocity is greater than critical velocity, as the result shown in Fig. 1(b) with U=1.9 m/s, the amplitude of vibration increases and tends to a limited value for sufficient long time. The iced conductor galloping occurs when wind velocity is greater than critical wind velocity.

The approximate value of galloping amplitude was also derived analytically by using Multi scale method. The positive real amplitude is plotted in Fig.3. It is easy seen that the critical velocity of galloping is coincide with that obtained by stability analysis. If the wind velocity is less than critical wind velocity, the iced conductor is always stable with the vibration amplitude a=0. On the contrary, if wind velocity is great than the critical wind velocity, the iced conductor gossiping occurs with nonzero amplitude. With the increase of wind velocity, the galloping amplitude

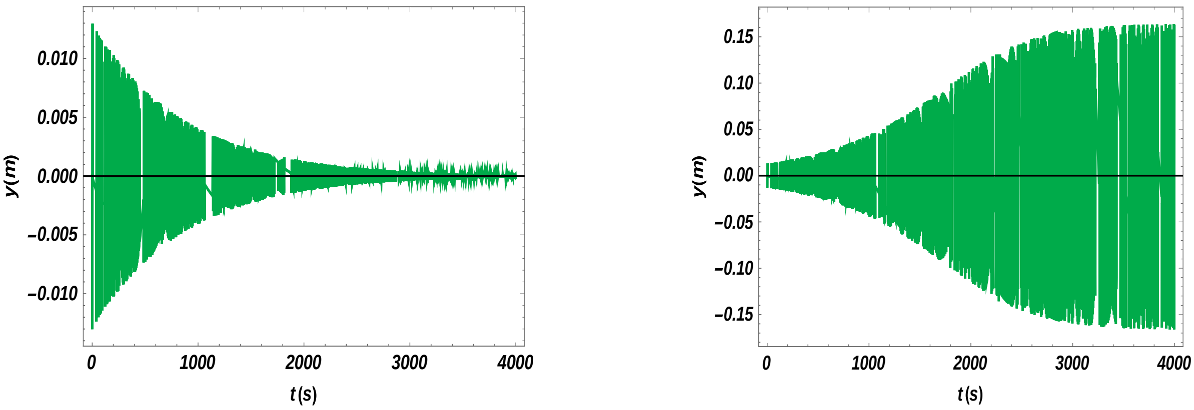

(a) (b)

Fig. 2 Vertical displacement with different wind velocities: (a) U=1.6m/s; (b) U=1.9m/s

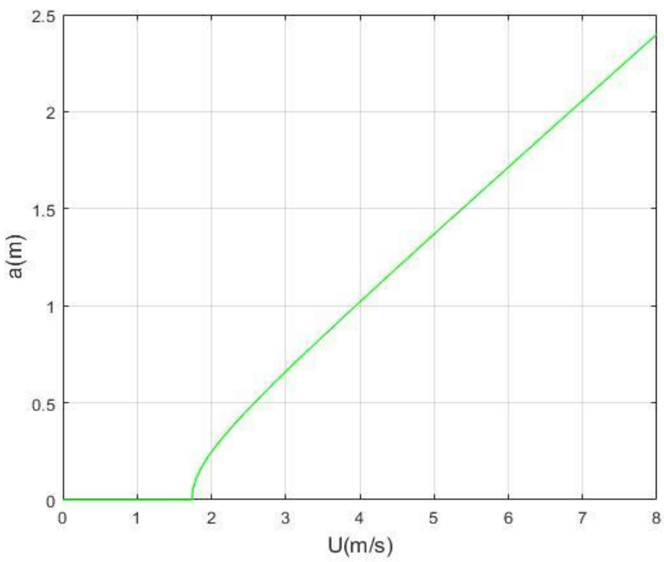

Fig. 3 The amplitude of the iced conductor with different wind velocity

Table 1 Parameters of the iced conductor

Parameter	Value	Dimension	Description
L	126	m	Span length
D	0.03	m	Diameter
E	4.78E10	N/m^2	Elastic Modulus
M	2.99	Kg/m	Mass per unit length
ξ_y	0.005	--	Damping ratio
T	30000	N	Initial tension

increases. The analytical results in Fig. 3 can be verified by directly solving the equations of motion in the time domain. Two wind velocities, U=3.5m/s and U=7.0m/s, were selected to verify the galloping amplitude. The phase trajectories of the iced conductor for different wind velocity were calculated and presented in Fig. 4. It is shown that both phase trajectories in Fig.4 tend to limited cycles. When U=3.5m/s, the vibration amplitude is about 0.8m. When U=7.0m/s, the vibration amplitude is 2.0m. These results coincide with those in Fig. 3. It is also seen that the midpoint of the motion is drifted with respect to the initial configuration, as predicted in second order approximation in Eq. (49). The galloping response of the iced conductor can be accurately predicted by using multi-scale method.

Some results were also obtained for iced conductor under turbulent wind. The fluctuation wind velocity was modelled as Gaussian white noise with intensity $\gamma^2 = 0.04$. As described in Section 4.1, the fluctuation wind velocity has little effect on the critical galloping wind velocity. The Monte Carlo Simulation (MCS) method (Sun 2006) was used to verify the analytical results. The vertical displacements were shown in Fig.5. The vertical displacement with mean wind velocity U=1.6m/s is shown in Fig. 5(a). The vibration amplitude of the conductor tends to zero with sufficient long time. It means that galloping does not occur when the mean wind velocity is less than critical wind velocity. However, when the mean wind velocity is greater than critical wind velocity, as the result shown in Fig. 5(b) with U=1.9m/s, galloping occurs and the amplitude tends to a limited value. Its seen that the fluctuation wind have not significant effect on critical wind velocity when the intensity of random fluctuation wind is weak and damping ratio of the iced conductor is small.

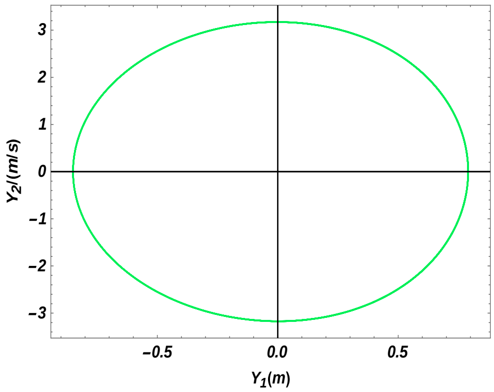

(a)

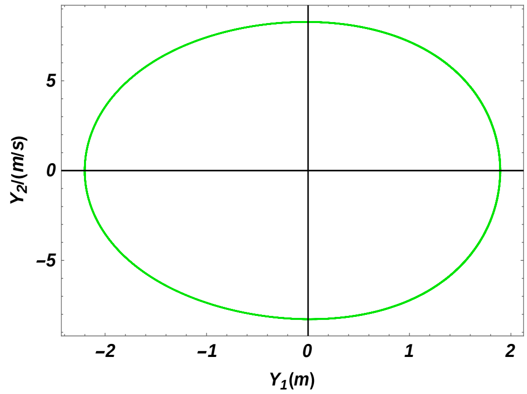

(b)

Fig. 4 Phase trajectory with different wind velocities: (a) U=3.5m/s; (b) U=7.0m/s

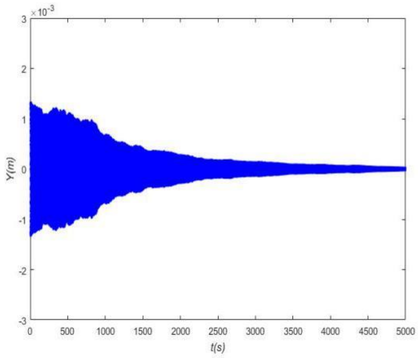

(a)

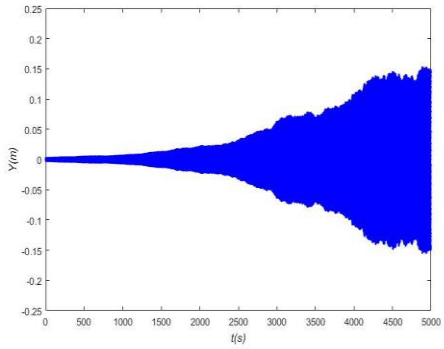

(b)

Fig. 5 Vertical displacement with different wind speeds: (a) U=1.6m/s; (b) U=1.9m/s

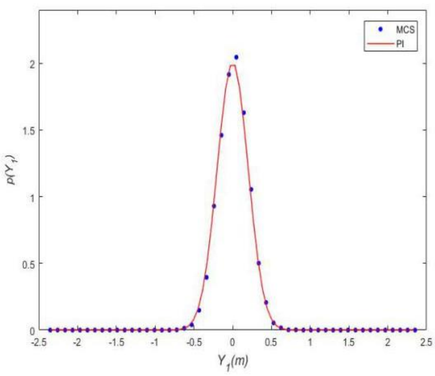

(a)

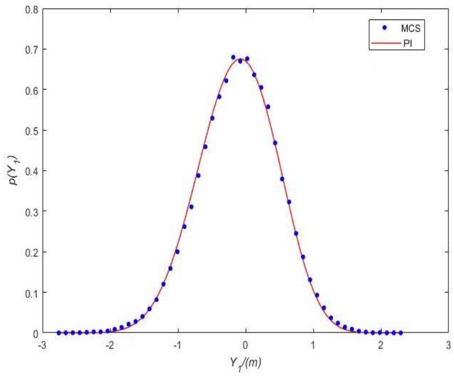

(b)

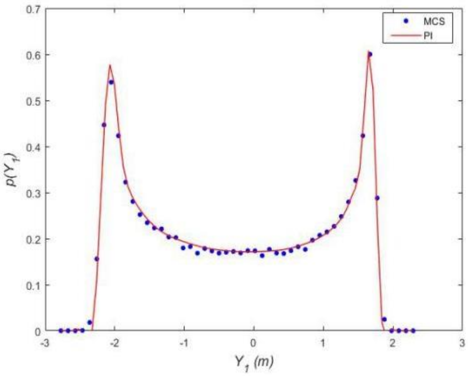

(c)

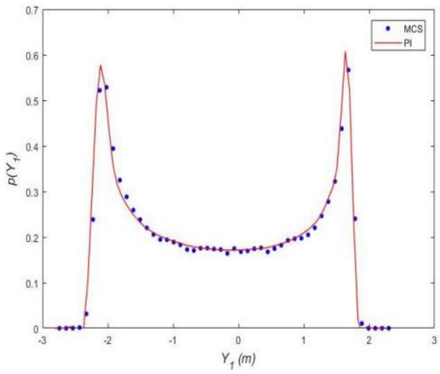

(d)

Fig. 6 Probability density of displacement at different time: (a)30s,(b)60s,(c)90s, (d)120s

The response of iced conductor under turbulent wind was calculated by using path integral method. The transient response and stationary response are shown in Fig.6 with mean wind velocity U=7.0m/s. Assuming that the iced conductor is in static state when t=0, the probability density of displacement Y_1 is plotted in Fig. 6 with different time t=30s, 60s, 90s and 120s. The vibration amplitude is small in short time. As time becomes longer, the vibration amplitude grows larger. Eventually, the probability density of displacement Y_1 reaches stationary state. It is shown that the galloping amplitude under turbulence wind exceeds the galloping amplitude under uniform wind. The tension of iced conductor under turbulence wind is larger than that under uniform wind. It can also be seen from these figures that the probability distribution of displacement is not symmetrical with respect to zero point. This asymmetry phenomenon corresponds to the drift of the midpoint of the motion respect to the initial configuration under uniform wind. The results obtained from Monte Carlo simulation are coincide with those obtained from path integral method.

6. Conclusions

The stability and response of iced conductor under both uniform wind and turbulent wind have been studied in this work. Considering that the initial configuration of an iced conductor is a suspension line, a nonlinear dynamic model is established to describe the motion of iced conductor galloping. In the case under uniform wind, the stability and critical wind velocity of iced conductor galloping have been derived by computing the eigenvalue of the linearized matrix; The first order and second order approximation of galloping amplitude have been obtained using multi-scale method. In the case under fluctuating wind, the necessary and sufficient conditions of the stability for iced conductor has been derived by using the Lyapunov exponent of the averaged system; The response the galloping conductor described by the probability density of displacement has been obtained by using the path integral method. The results in numerical example verify the effectiveness of the previous methods. The fluctuating characteristics of the wind have little influence on the stability of the iced conductor. Using the theory of uniform wind to study the stability of the iced conductor is accurate enough. However, the fluctuating wind has a great influence on the amplitude of the galloping of iced conductor, because the fluctuating wind may cause the iced conductor to vibrate greatly in a certain probability. Large vibration amplitude is easy to cause the damage of iced conductor.

Acknowledgments

The research described in this paper was financially supported by National Key R&D Program of China (Grant No. 2017YFC0803300) and the National Natural Science Foundation of China (Grant No. 11772277).

References

Cai, G.Q. and Zhu, W.Q. (2017), *Elements of Stochastic Dynamics*, World Scientific Co. Pte. Ltd., Singapore.

Chadha, J. and Jaster, W. (1975), "Influence of turbulence on the galloping instability of iced conductors", *IEEE Trans. Power App. Syst.*, **94**(5),1489-1499. https://doi.org/10.1109/T-PAS.1975.31991.

Choi, E.Y., Cho, J.R., Cho, Y.U., Jeong, W.B., Lee, S.B., Hong, S.P. and Chun, H.H. (2015), "Numerical and experimental study on dynamic response of moored spar-type scale platform for floating offshore wind turbine", *Struct. Eng. Mech.*, **54**(5), 909-922. https://doi.org/10.1109/T-PAS.1975.31991.

Den Hartog, J.P. (1932). "Transmission line vibration due to sleet", *AIEE Tran.*, **51**(4), 1074-1086. https://doi.org/10.1109/T-AIEE.1932.5056223.

Desai, Y.M., Yu, P., Popplewell, N., and Shah, A.H. (1995). "Finite element modeling of transmission line galloping", *Comput. Struct.*, **57**(3), 407-420. https://doi.org/10.1016/0045-7949(94)00630-L.

Irvine, H.M., and Caughey, T.K. (1974). "The linear theory of free vibration of a suspended cable", *Philos. T R Soc. A.*, **641**, 299-315. https://doi.org/10.1098/rspa.1974.0189.

Kim, J.W. and Sohn, J.H. (2018), "Galloping simulation and of the power transmission line under the fluctuating wind", *Int. J. Precis. Eng. Manuf.*, **19**(9), 1393-1398. https://doi.org/10.1007/s12541-018-0164-2.

Lin L., Ang A.H.S., Xia D.D., Hu H. T., Wang H.F. and He F.Q. (2017), "Fluctuating wind field analysis based on random Fourier spectrum for wind induced response of high-rise structures", *Struct. Eng. Mech.*, **63**(6), 837-846. https://doi.org/10.12989/sem.2017.63.6.837.

Lin, Y.K. and Cai G.Q. (1995), *Probabilistic Structural Dynamics*, McGraw-Hill Inc., New York, NY, USA.

Lou, W.J., Yang L. Huang M.F. and Yang X.H. (2014), "Two-parameter bifurcation and stability analysis for nonlinear galloping of Iced transmission lines", *J. Eng. Mech.*, **140**(11), 04014081. https://doi.org/10.1061/(ASCE)EM.1943-7889.0000795.

Macdonald J., Larose G. (2006), "A unified approach to aerodynamic damping and drag/lift instabilities and its application to dry inclined cable galloping", *J. Fluid. Struct.*, **22**(2), 229-252. https://doi.org/10.1016/j.jfluidstructs.2005.10.002.

Naess A. and Moe V. (2000), "Efficient path integration methods for nonlinear dynamic systems", *Probabilistic Eng. Mech.*, **15**, 221-231. https://doi.org/10.1016/S0266-8920(99)00031-4.

Nayfeh, A.H., and Mook D.T. (1995), *Nonlinear Oscillations,* John Wiley Sons Inc., New York, NY, USA.

Nayfeh, A.H., Arafat, H.N., Chin, C.M., and Lacarbonara, W. (2002), "Multimode interactions in suspended cables", *J. Vib. Control*, **8**(3), 337–387. https://doi.org/10.1177/107754602023687.

Nigol, O. and Buchan, P.G. (1981), "Conductor Galloping 2: Torsional mechanism", *IEEE Trans. Power App. Syst.*, **100**(2), 708-720. https://doi.org/10.1109/TPAS.1981.316922.

Petrini F., Olmati P. and Bontempi (2019), "Coupling effects between wind and train transit induced fatigue damage in suspension bridges", *Struct. Eng. Mech.*, **70**(3), 311-324. https://doi.org/10.12989/sem.2019.70.3.311.

Sun J.Q. (2006), *Stochastic Dynamics and Control*, Elsevier, Amsterdam, The Netherlands.

Van Dyke, P., and Laneville, A. (2008). "Galloping of a single conductor covered with a D-Section on a high-voltage overhead test line", *J. Wind Eng. Ind. Aerodyn*, **96**(6-7), 1141-1151. https://doi.org/10.1016/j.jweia.2007.06.036.

Wang, J. and Lilien, J.L. (1998). "Overhead electrical transmission line galloping: A full multi-span 3-DOF model, some applications and design recommendations", I*EEE Trans. Power Deliv.*, **13**(3), 909-916. https://doi.org/10.1109/61.686992.

Yu, P., Shah, A. H. and Popplewell, N. (1992), "Inertially coupled galloping of iced conductors", *J. Appl. Mech*., **59**(1), 140-145. https://doi.org/10.1115/1.2899419.

Yu, P., Desai, Y. M., Popplewell, N. and Shah, A. H. (1993), "Three-degree-of-freedom model for galloping. Part II: Solutions", *J. Eng. Mech*., https://doi.org/10.1061/(ASCE)0733-9399(1993)119:12(2426), 2426–2448.

Zhang, J.F., Liu, Q.S., Ge, Y.J. and Zhao, L. (2019), "Studies on the influence factors of wind dynamic responses on hyperbolic cooling tower shells", *Struct. Eng. Mech*., **72**(5), 541-555. https://doi.org/10.12989/sem.2019.72.5.541.

Zhi L.H., Chen B. and Fang M.X. (2015), "Wind load estimation of super-tall buildings based on response data", *Struct. Eng. Mech*., **56**(4), 625-648. https://doi.org/10.12989/sem.2015.56.4.625.

CC

Appendix

$a_1 = \int_0^L M\phi^2(x)\,dx$, $a_2 = \int_0^L 2M\omega_y\xi_y\phi^2(x)\,dx$, $a_3 = \int_0^L (T + EAy_x^2)\phi_x^2(x)\,dx$,
$a_4 = \frac{3}{2}\int_0^L EAy_x\phi_x^3(x)\,dx$, $a_5 = \int_0^L \frac{1}{2}EA\phi_x^4(x)\,dx$, $F_y = \int_0^L f_y(x,t)\phi(x)\,dx$,
$b_1 = \frac{1}{a_1}\int_0^L \frac{1}{2}\rho DU\hbar_1\phi^2(x)\,dx$, $b_2 = \frac{1}{a_1}\int_0^L \frac{1}{2}\rho D\hbar_2\phi^3(x)\,dx$,
$b_3 = \frac{1}{a_1}\int_0^L \frac{1}{2U}\rho D\hbar_3\phi^4(x)\,dx$,
$c = \dfrac{a_2}{a_1} = 2\omega_y\xi_y, k_1 = \omega_y^2 = \dfrac{a_3}{a_1}, k_2 = \dfrac{a_4}{a_1}, k_3 = \dfrac{a_5}{a_1}.$